proceedings

MDPI

Proceedings

Fourier-Transform Infrared Microspectroscopy (μFT-IR) Study on *Caput* and *Cauda* Mouse Spermatozoa†

Marianna Portaccio, Sonia Errico, Teresa Chioccarelli, Gilda Cobellis and Maria Lepore *

Dipartimento di Medicina Sperimentale, Università della Campania "L. Vanvitelli", 80138 Naples, Italy; marianna.portaccio@unicampania.it (M.P.); sonia.errico@unicampania.it (S.E.); teresa.chioccarelli@unicampania.it (T.C.); gilda.cobellis@unicampania.it (G.C.)

* Correspondence: maria.lepore@unicampania.it

† Presented at the 6th International Electronic Conference on Sensors and Applications, 15–30 November 2019; Available online: https://ecsa-6.sciforum.net/

Published: 14 November 2019

Abstract: Fourier-Transform Infrared micro-spectroscopy (μFT-IR) was used for an in vitro investigation on spermatozoa (SPZ) samples separately collected from *caput* and *cauda* of mouse epididymis. SPZ are characterized by deep biochemical changes during the transit along the epididymis and they can constitute ideal candidates for a μFT-IR investigation thanks to the ability of this technique in analyzing cells at a molecular level. Appreciable differences were reported in the infrared spectra from *caput* and *cauda* SPZ and biochemical changes in protein, nucleic acid, lipid, and carbohydrate content of cells were evidenced. The present investigation indicates that μFT-IR can constitute a valuable tool for monitoring in an easy and fast way the changes suffered by SPZ during the transit along the epididymis.

Keywords: *caput* and *cauda* spermatozoa; μFT-IR microspectroscopy; protein; nucleic acid; lipid; and carbohydrate components.

1. Introduction

Fourier transform IR (FT-IR) spectroscopic technique is nowadays a very valuable tool for the nondestructive analysis of biological specimens. FT-IR results particularly useful in cytological and histological diagnosis also by using imaging procedures [1]. FT-IR is able to reveal bonds presenting a change of dipole moment during vibrational motion. These vibrational modes can be quantitatively characterized by IR spectroscopy, providing a very sensitive, label-free tool for studying molecular composition and dynamics without perturbing the sample. When FT-IR spectroscopy is performed on biological materials, the most important spectral regions are the fingerprint region (600–1450 cm^{-1}) and the amide I and amide II (amide I/II) region (1500–1700 cm^{-1}). The higher-wavenumber region (2800–3500 cm^{-1}) is due to stretching vibrations such as S-H, C-H, N-H and O-H, whereas the lower-wavenumber regions typically correspond to bending and carbon skeleton fingerprint vibrations. These regions are able to give a complete biochemical fingerprint of the structure and function of investigated samples and have been adopted in a very large number of different samples of biological interest.

Recently, FT-IR spectroscopy has been adopted for investigating spermatozoa (SPZ) samples in order to principally take advantage of its non-invasivity. In particular, cyanide toxicity effects on rat sperms have been investigated at a molecular level by using FT-IR technique. Cyanide compounds are largely used in industries and are considered to be a ubiquitous pollutant in the environment. The use of FT-IR spectroscopy has also allowed an investigation on the secondary structure of protein

components. It is worth to note that a complementary vibrational technique, the Raman one, has been used for investigating oxidative DNA damage in human sperm [2].

In the present paper, FT-IR microspectroscopy (μFT-IR) has been adopted for characterizing SPZ separately collected from *caput* and *cauda* of the epididymis. Interestingly, SPZ are transcriptionally and translationally silent cells. During the epididymal transit, from *caput*-to-*cauda*, these cells undergo maturation via massive biochemical changes [3,4] that include: (i) decreases of cholesterol; (ii) qualitative composition of cytoplasmic proteins and RNA, (iii) protein degradation and phosphorylation; (iv) acquisition of GPI-anchored membrane proteins; (v) proteolytic remodelling of membrane proteins, (vi) fatty acid composition from saturated to polyunsaturated forms, (vii) DNA methylation, (viii) inter/intra protamine disulfide-bound formation. Because of their remarkable biochemical differences, *caput* and *cauda* SPZ can be considered ideal candidates for an FT-IR spectroscopy investigation.

In this report, we summarize the preliminary results of an investigation on mouse sperm samples from *caput* and *cauda* epididymis. To our knowledge, this is the first time that vibrational spectroscopies are adopted for investigating the changes occurring in SPZ during the epididymal transit.

2. Materials and Methods

2.1. Collection of Sperm Samples from Caput and Cauda Epididymis

Adult male mice (CD1 background, from Charles River Laboratories, Lecco, Italy) were euthanized by asphyxia with CO2 and epididymis were dissected for sperm collection. Briefly, caput and cauda epididymis were separately immersed in PBS (pH 7.6) and slightly cut to endorse sperm extrusion from the epididymal duct, as previously reported [5]. Spermatozoa samples, separately collected from *caput* and *cauda* epididymis, were filtered throughout cheesecloth, washed by centrifugation (200xg for 5 min), in 0.9% NaCl solution and pellets were processed for FT-IR analysis.

All animal studies were carried out in accordance with the principles and procedures outlined in the National Institute of Health Guide for Care and Use of Laboratory Animals and approved by the Italian Ministry of Research and the Italian Ministry of Health.

2.2. FT-IR Spectral Analysis

For FT-IR spectral analysis SPZ pellets were resuspended in 0.9% NaCl solution and drops of few microliters were used for spectra acquisition. For this purpose, a Perkin Elmer Spectrum One FT-IR spectrometer equipped with a Perkin Elmer Multiscope system infrared microscope (Mercury Cadmium Telluride detector) was used. Spectral acquisitions were performed in specular-reflection mode with thin layers of samples (2 μL) put on metallic IR-reflective surface. The background spectrum was collected from the metallic IR-reflective surface without sample. A sampling spot on the surface was selected through an objective (l0X optical or 15X infrared). All spectra were collected using 64 scans in the range from 4,000 to 600 cm^{-1} with a 4 cm^{-1} spectral resolution.

The spectra were preliminarily analyzed using the application routines provided by the software package ("Spectrum" User Guide, Perkin Elmer Inc. USA) controlling the whole data acquisition system. "Spectrum" (release 5.0.2, 2004) is the main Perkin Elmer software package for collecting, viewing and processing IR spectra.

3. Results and Discussion

The μFT-IR average spectra of mouse SPZ samples from *caput* and *cauda* epididymis (*caput* and *cauda* SPZ) were obtained in the 4000-600 cm^{-1} range. The peak position and band assignments were done in agreement with ref. 6. In order to evidence the differences occurring between the two spectra, they were divided into four wavenumber ranges: 3600–3000 cm^{-1} (Figure 1), 3050–2800 cm^{-1} (Figure 2), 1800–1200 cm^{-1} (Figure 3) and 1200–600 cm^{-1} (Figure 4).

Figure 1 shows the average μFT-IR spectra of *caput* and *cauda* SPZ in the range of 3600–3000cm^{-1}. In this range, there is the large contribution of amide A band (located at 3309 and 3290 for *caput* and

cauda SPZ, respectively) due to N-H and O-H stretching modes of proteins and intermolecular H bonding. It is worth to note that the shape of this band changes between *caput* and *cauda* samples. In particular, for *caput* SPZ the maximum is located at ~3400 cm^{-1}, conversely, for *cauda* SPZ, the maximum is located 3290 cm^{-1}. A very weak contribution ~3070 cm^{-1} can be noticed only in the case of *cauda* samples and can be attributed to the N-H stretching of amide B. In order to analyze the changes in the lipid content of *caput* and *cauda* SPZ, the spectral region from 3050 to 2800 cm^{-1} was considered (Figure 2). In this region, it is possible to evidence the contributions of CH_3 asymmetric stretching (located at 2957 and 2959 cm^{-1} for *caput* and *cauda* samples, respectively), CH_2 asymmetric stretching (located at 2922 and 2924 cm^{-1} for *caput* and *cauda* samples, respectively), CH_3 symmetric stretching (located at 2875 cm^{-1} for both *caput* and *cauda* samples) and CH_2 symmetric stretching (located at 2851 and 2853 cm^{-1} for *caput* and *cauda* samples, respectively). It's important to note that the two spectra are largely different in shape and relative intensity of the main peaks even though the position of the different CH_2 and CH_3 contribution do not change in a crucial way. In particular, the position of CH_2 symmetric stretching doesn't show significant changes taking into account the spectral resolution of our equipment (4 cm^{-1}). This can indicate that no important changes in membrane fluidity occur [7]. In this region of the spectra, it is also present a contribution at 3013 cm^{-1} that is more evident for *caput* SPZ samples. This band is usually assigned to olefinic functional group in unsaturated lipids, mainly due to C-H stretching mode. This band can be used for further investigating lipid peroxidation in tissue [8].

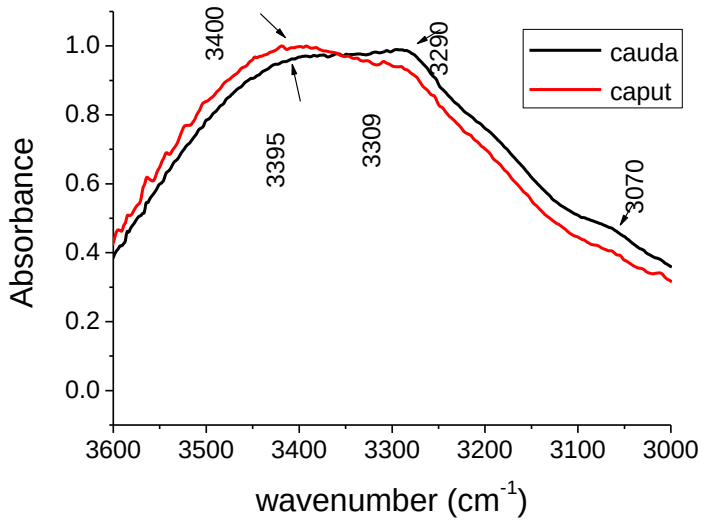

Figure 1. FT-IR spectra of caput and cauda sperm of WT mouse in 3600–3000 cm^{-1} region.

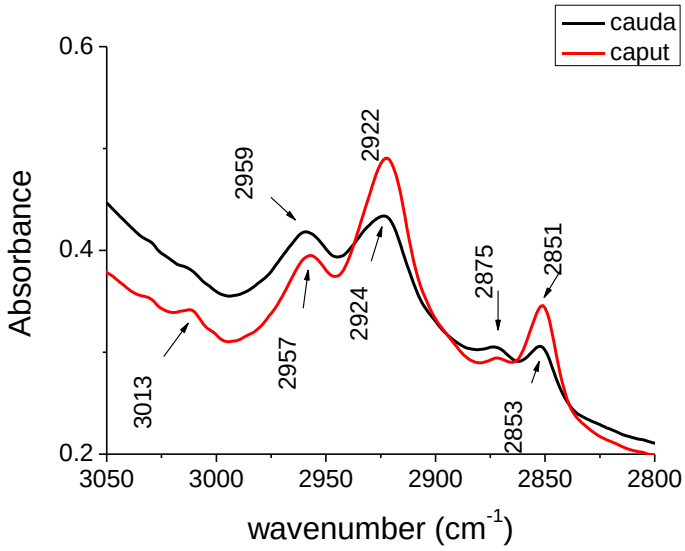

Figure 2. FI-IR spectra of caput and cauda sperm of WT mouse in 3050–2800 cm^{-1} region.

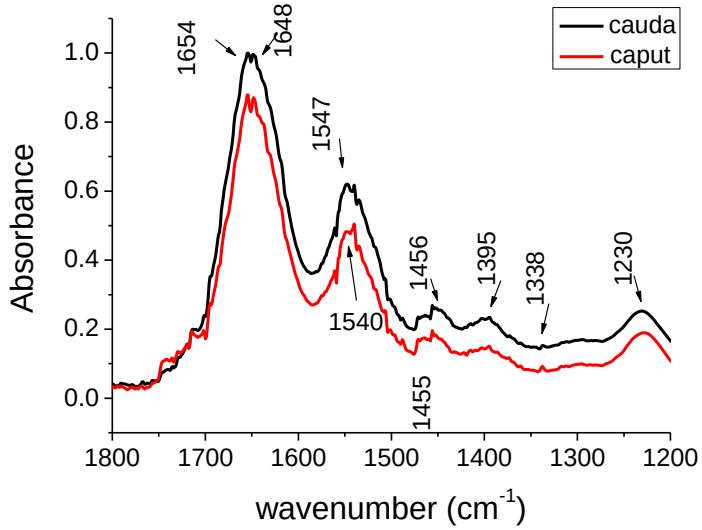

Figure 3. FI-IR spectra of caput and cauda sperm of WT mouse in 1800–1200 cm^{-1} region.

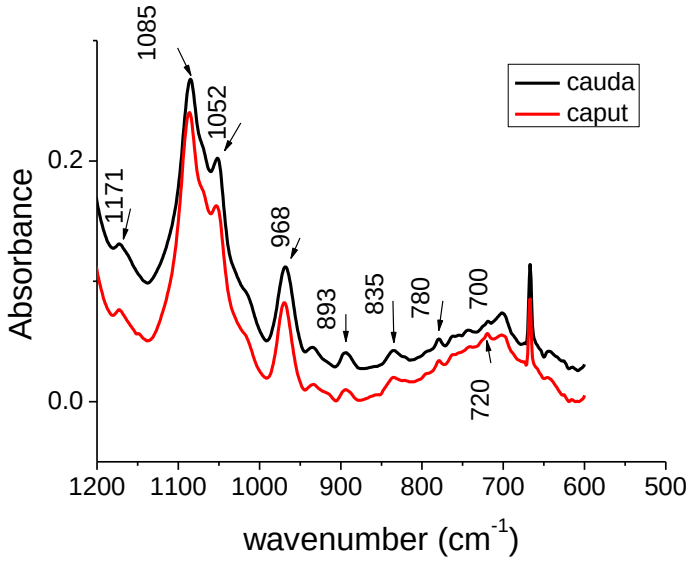

Figure 4. FI-IR spectra of caput and cauda sperm of WT mouse in 1200–600 cm^{-1} region.

In Figure 3 the 1800-1200 cm^{-1} region of μFT-IR spectra of *caput* and *cauda* SPZ is reported. In this region, the main contributions are due to protein content. In particular, the band due to the Amide I C=O stretching is positioned ~1650 cm^{-1} for the two different samples, but differences can be noted in the band's shape. In Figure 3, the contributions of Amide II (at 1540 and 1547 cm^{-1} for *caput* and *cauda* samples, respectively) and Amide III (at 1300 cm^{-1} for both *caput* and *cauda* samples) are present. The small band positioned at 1455 and 1456 cm^{-1} for *caput* and *cauda* samples, respectively can be due to CH_3 asymmetric bending and CH_2 scissoring mode that can be associated with lipid and protein contents. At 1395 cm^{-1} a small feature can be noticed and it can be attributed to COO^- symmetric stretching vibration mode related to fatty acids. The band located at 1230 cm^{-1} is due to PO_2^- asymmetric stretching mode related to nucleic acids and phospholipids contributions.

In Figure 4 the region of short wavenumber (1200-600 cm^{-1}) of μFT-IR spectra of *caput* and *cauda* SPZ is shown. This region is mainly related to DNA contributions. The most important ones are located at 1085 (PO_2^- symmetric stretching) and 1052 cm^{-1} (C–O stretching). In this region too, differences can be noted in the band shape. Also the other structures positioned at 968 cm^{-1} (C–C stretching), 893 cm^{-1} (deoxyribose ring), 835 cm^{-1} (S- type sugar) are attributed to DNA. A complete list of the peak position and band assignments is reported in Table 1.

Table 1. Mode assignments for the FT-IR frequency values in caput and cauda sperm samples, abbreviation: as = asymmetric, s = symmetric, ν = stretching, vbr = vibration, b = bending, scis = scissoring.

Peak *caput* cm^{-1}	Peak *cauda* cm^{-1}	Peak Assignments	Biochemical Molecules
3400	3395	Hydrogen bonded O-H ν N-H ν	protein water
3309	3290	Amide A (N-H ν)	protein
3013	3013	olefinic =C-H ν	unsaturated lipid
2957	2959	CH_3 as ν	lipid
2922	2924	CH_2 as ν	lipid
2875	2875	CH_3 s ν	lipid

2851	2853	CH_2 s ν	lipid
1654	1654	Amide I α-helix	protein
1648	1648	Amide I	protein
1540	1547	Amide II	protein
1455	1456	CH_3 as b CH_2 scis	lipid and protein
1395	1395	COO- s ν	fatty acid
1300	1300	Amide III	protein
1230	1230	PO_2- as ν	nucleic acids and phospholipids
1171	1171	CO-O-C ν	glycogen
1085	1085	PO_2- s ν	nucleic acids
1052	1052	C-O ν	saccharides and DNA deoxyribose
968	968	C-C ν	DNA backbone
893	893	Deoxyribose ring	DNA
835	835	DNA S-type sugar	DNA

4. Conclusions

The results here reported indicate that μFT-IR spectroscopy can constitute a useful tool for investigated changes occurring in SPZ from *caput* and *cauda* epididymis of mouses in a rapid and easy way. Biochemical changes in protein, nucleic acid, lipid, and carbohydrate content of cell have been evidenced. Further work is in progress in order to quantitatively assess the observed differences.

Acknowledgments: This work was supported by Università della Campania "L. Vanvitelli" (Italy) under the project "Ricerca Scientifica di Dipartimento" (2017). The authors are pleased to thank Nadia Diano for useful discussions.

Compliance with ethical standards: All applicable international, national, and/or institutional guidelines for the care and use of animals were followed.

Conflicts of Interest: The authors declare that there is no conflict of interest.

References

1. Baker, M.J. et al.; Using Fourier transform IR spectroscopy to analyze biological materials. *Nat. Protoc*. **2014**, *9*, 1771–1791.
2. Shivanoor, S.M.; David,M. Fourier transform infrared (FT-IR) study on cyanide induced biochemical and structural changes in rat sperm. *Toxicology Reports* **2015**, *2*, 1347–1356.
3. Sánchez, V.; Redmann, K.; Wistuba, J.; Wübbeling, F.; Burger, M.; Oldenhof, H.; Wolkers, W.F.; Kliesch, S.; Schlatt, S.; Mallidis, C. Oxidative DNA damage in human sperm can be detected by Raman microspectroscopy. *Fertil. Steril.* **2012**, *98*, 1124–1129.
4. Marciani, S.; Tamburrino, L.; Muratori, M.; Baldi, E.: Epididymal sperm transport and fertilization. In: *Endocrinology of the Testis and Male Reproduction Endocrinology 1;* Simoni, M., Huhtaniemi, I.T. (eds.). Springer International Publishing AG, 2017, pp. 457–478.
5. Cooper, T.G. Epididymis. In *Enciclopedia of Reproduction,* Knobil, E.; Neill, J.D. (Eds), Academic Press 2003**,** pp.1-17.
6. Portaccio, M.; d'Apuzzo, F.; Perillo, L.; Grassia, V.; Errico, S.; Lepore, M. Infrared microspectroscopy characterization of gingival crevicular fluid during orthodontic treatment. *Journal of Molecular Structure* **2019**, *1176*, 847–854.
7. Liu, K.Z.; Schultz, C.P.; Mohammad, R.M.; Johnston, J.B.; Mantsch, H.H. Infrared spectroscopic study of bryostatin 1-induced membrane alterations in a B-CLLcell line. *Leukemia* **1999**, *13*, 1273–1280.

8. Severcan, F.; Gorgulu, G.; Gorgulu, S.T.; Guray, T. Rapid monitoring of diabetes-induced lipid peroxidation by Fourier transform infrared spectroscopy: Evidence from rat liver microsomal membranes. *Anal. Biochem.* **2005**, *339*, 36–40.